

Hydrokinetic Power Generation System coupled to the Axial-Flow Generator

Viviane Barrozo da Silva¹, Fernando Jakitsch Medina², Fábio Monteiro Steiner³, Afrânio de Castro Antonio⁴, Antonio Carlos Duarte Ricciotti⁵, Hebert Sancho Garcez Militão⁶, Júlio Sancho Teixeira Militão⁷, Daniela de Araújo Sampaio⁸, Petrus Luiz de Luna Pequeno⁹

^{1,5}Department of Electrical Engineering, Federal University of Rondonia, Brazil

⁷Department of Chemistry, Federal University of Rondonia, Brazil

^{4,6}Control and Automation Laboratory, Rondonia, Brazil

⁹Department of Civil Engineering, Federal University of Rondônia, Brazil

⁸Department of Food Engineering, Federal University of Rondonia, Brazil

^{2,3}EDF Norte Fluminense, Brazil

¹E-mail: viviane-barrozo@unir.br

Received: 15 Jun 2021;

Received in revised form: 11 Jul 2021;

Accepted: 20 Jul 2021;

Available online: 29 Jul 2021

©2021 The Author(s). Published by AI
Publication. This is an open-access article
under the CC BY license
(<https://creativecommons.org/licenses/by/4.0/>).

Keywords— *low speeds, Converter, Axial Flow, Generator.*

Abstract— *Decentralized power generation is an option to serve communities that survive in places without electricity or isolated from urban centers or in areas with intermittent electricity coming from gasoline or diesel generator sets. This article presents an alternative energy generation with low environmental and financial impact, a floating hydroelectric generation system using an axial flow electric generator combined with a cross-flow hydrokinetic converter that works from water flows in rivers' sections floating structure allows for performance even at low speeds.*

I. INTRODUCTION

Electricity is needed to develop isolated regions of the country, as access to this service is vital in economic and social development, impacting people's communication, productive use, and a direct relationship to improving the quality of life [4].

The high costs of transmission lines can be caused by the large distances between homes to the network due to the low population density in the Amazon region [4].

Alternative decentralized service solutions have been encouraged by the federal government through social programs. These programs aim to bring electricity to rural regions, isolated through micro and mini hydroelectric plants, thermoelectric plants powered by biofuels or

natural gas, solar photovoltaic plants, wind turbines, hybrid systems [3], [4].

The proposed Hydrokinetic Power Generation System coupled to the Axial-Flow Generator may be a viable option for communities close to rivers with specific hydrological characteristics, including a frequent and constant water flow. This generation system is robust, easy to maintain, and with low financial investment and no environmental impact, as it does not use large, flooded areas.

II. MODELING OF THE HYDROKINETIC GENERATION SYSTEM COUPLED TO THE AXIAL FLOW GENERATOR

Michell-Banki-type cross-flow turbines use a drum-type rotor equipped with blades. The water flow is directed by a hydraulic profile and meets the rotor blades, driving it. This type of turbine is used in hydraulic projects with smaller waterfalls and a greater volume of excellent water, which usually occurs in flatter regions. [1], [3].

The various types of couplings used between the converter and the generator result in problems ranging from balancing the axes, exposure of the parts to weather, more significant space used, and even maintenance [3].

The construction of unique equipment, which combines a cross-flow hydro converter with a permanent magnet generator or squirrel cage induction motor in an axial flow machine, allows for space and maintenance gains and greater power [3]. The proposed system works submerged or in line with pipes where there are flows of any type [3], [5].

In [3] presents the mathematical modeling of the axial flow generator and the dimensioning of the permanent magnets.

The prototype will be installed on the Madeira River. One of the largest rivers in the world in terms of water volume. It has a total drainage area of 1,420,000 km², or about 1/5 of the entire Amazon basin.

The surveys were carried out with the National Water Agency (known in Brazil by its Portuguese acronym - ANA), in its database, and with the Mineral Resources Research Company (known in Brazil by its Portuguese acronym - CPRM) in Rondônia, where there is historical data on flow, flow velocity, and depth, were made available for consultation, enabling modeling and simulation for the elaboration of the construction project of the floating hydroelectric system in realist scale.

Fig.1 shows the installation location of the Hydrokinetic Power Generation System coupled to the floating Axial Flow Generator.



Fig.1: The Installation location of the proposed system.

The Madeira River is known for transporting a large amount of suspended material and, in the rainy season, its flow goes from 5,000 m³/s to 50,000 m³/s. Understanding the dynamics of the river, given this seasonality, is essential for determining the parameters of the floating hydroelectric system.

A large amount of sediments in the river increases the fluid density and, in a direct ratio, the available hydraulic power. However, the corrosion problems are more evident.

An important input parameter for the design of a hydrokinetic converter is the river flow velocity since the available hydraulic power is directly proportional to the section area and the cube of the flow velocity. This data over time becomes even more relevant in a river with significant variation in its regime, as is the case of the Madeira River, as shown in Fig. 2.

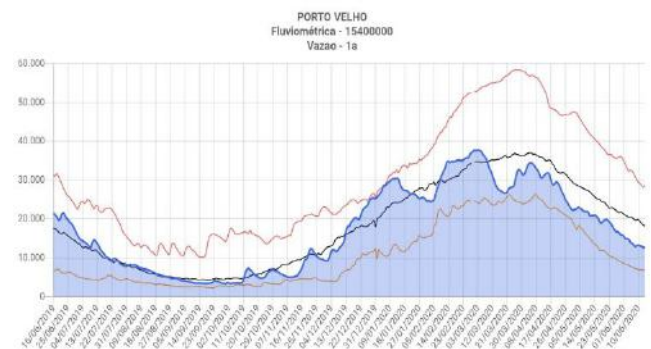


Fig.2: In red is a historical maximum, in orange historical minimum, and in blue the flow value of the last 12 months.

An ACDP - Acoustic Doppler Current Profiler is used to raise the current profile, a hydro-acoustic current profiler that measures the velocity of particles in the water column using a physical principle of propagation of sound waves (Doppler effect). This type of equipment is shown in Fig. 3.

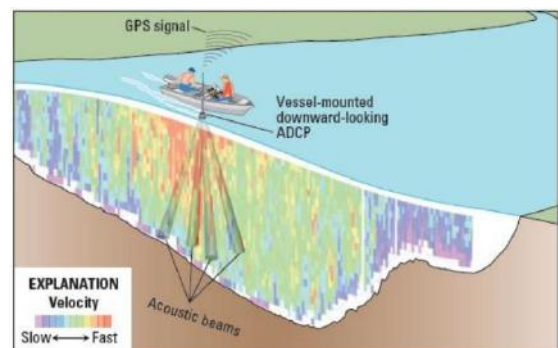


Fig.3: Functioning Acoustic Doppler Current Profiler [6].

The collected flow velocity historical data are simulated in the WinRiver II software, where it is possible

to observe the current velocity profile and the bed trace as shown in Figures. 4 and 5.

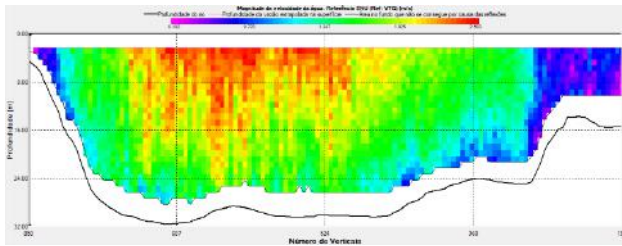


Fig.4: Typical measurement in the flood period (February 2020).

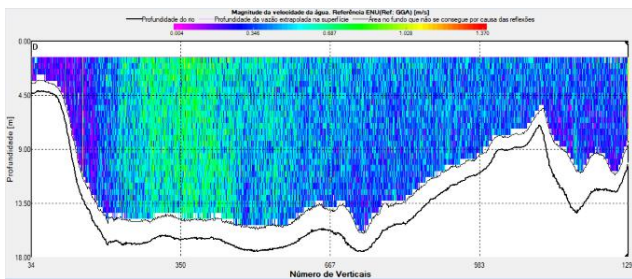


Fig.5: Typical measurement in the dry period (September 2016).

As shown in figures 4 and 5, the average velocity at 200 meters from the right bank of the Madeira River varies from 0.7 m / s in the dry period to 2.5 m / s in flood. With this data, it is possible to develop simulations of the river flow, including the floating system where the turbine will be located. Fig. 6 shows the flow simulation of a natural flow channel with the floating turbine housing system.

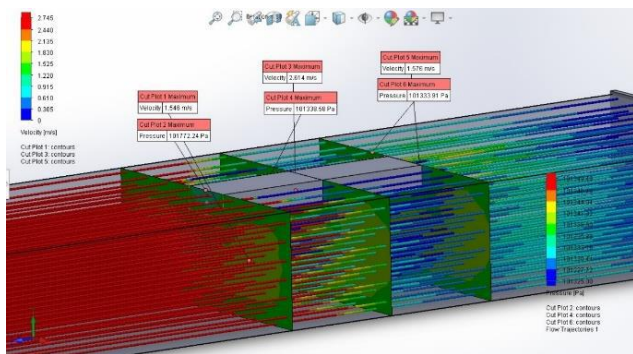


Fig.6: One-channel flow simulations.

A simulation of a diffuser to determine the energy available for a generation was presented in [3]. The results presented demonstrate an extensive recirculation below the diffuser. This recirculation is a hydraulic loss. A new diffuser geometry is proposed to solve this problem, according to the simulations presented in Figures 7, 8, 9, and 10.

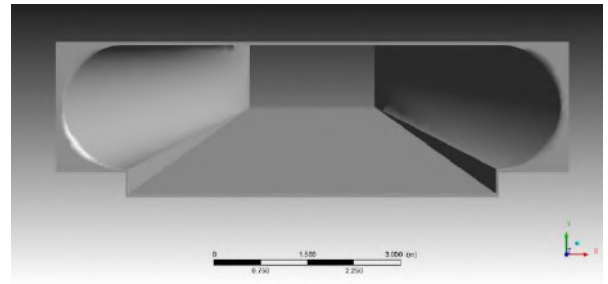


Fig.7: Front view of the diffuser.

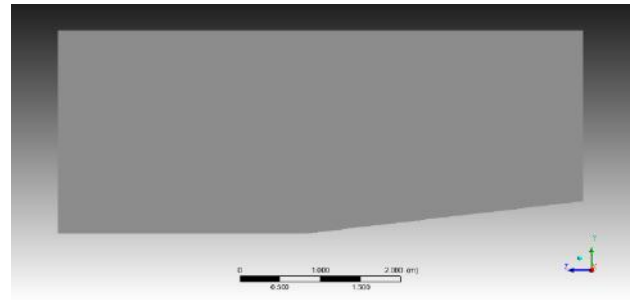


Fig.8: Side view of the diffuser.

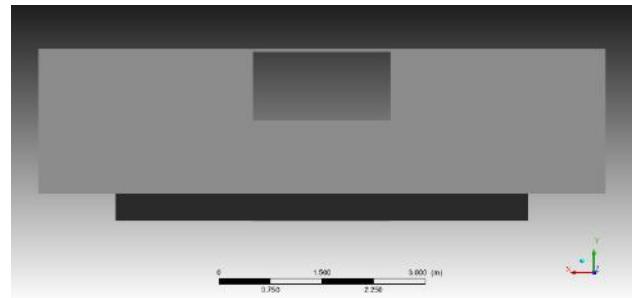


Fig.9: Rear view of the diffuser with exit window (rotor position).

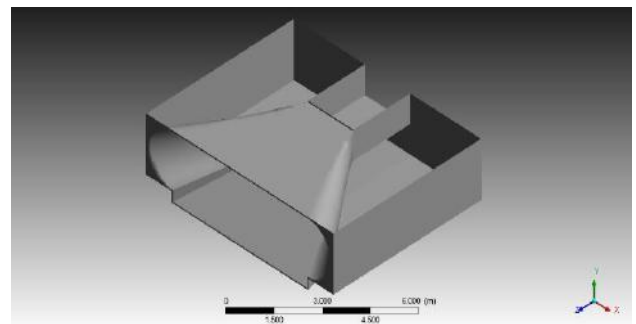


Fig.10: Isometric view of the diffuser.

The computational model used for simulation is shown in Fig. 11. The inflow (upstream), Fig. 12, was based on historical measurements of the speed of the Madeira River in Porto Velho – Rondônia. The geometry was worked on

the SpaceClaim software, Ansys Inc. 2017, and the Meshing software generated the mesh.

In the dry period, the average speed is around 0.7 m/s, and in the flood period, it is 2.5 m/s. Based on this history, the input speed was simulated from 0.5 to 3.0 m/s with an increment of 0.5 m/s.

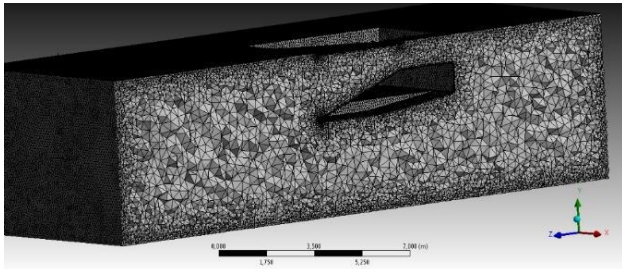


Fig.11: Computational model used for simulations.

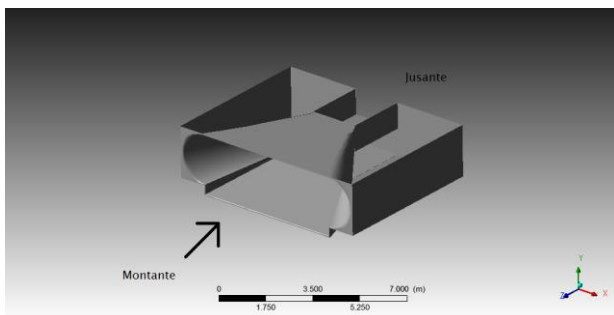


Fig.12: Computational model boundary conditions.

For numerical simulation, used the CFX software Ansys Inc. 2017. The parallel processing resource was used.

In Fig.12, the input boundary conditions (upstream) are presented along with the average speed obtained near the diffuser inlet and the average diffuser output speed.

In Table 1, the input boundary conditions (upstream) are presented along with the average velocity obtained near the diffuser inlet and the average diffuser exit velocity.

Table 1 - Speeds Obtained in the Computational Model

Input	Average input speed	Average output speed
3,0	2,880090	2,998580
2,5	2,400370	2,497730
2,0	1,920250	1,997130
1,5	1,440110	1,496750
1,0	0,959991	0,996668
0,5	0,479909	0,497159

The input velocity is the boundary condition imposed on the computational model, which, in turn, represents the historical average velocity measured in the Madeira River. Due to the flow pressure drop and viscous and kinetic effects, the speed decreases along the way. An average speed near the diffuser inlet (blue plane) was calculated, Fig. 13, which shows the details of the regions to obtain the average velocities.

The hydraulic potential across the diffuser is obtained by an average speed calculated at the outlet (yellow plane).

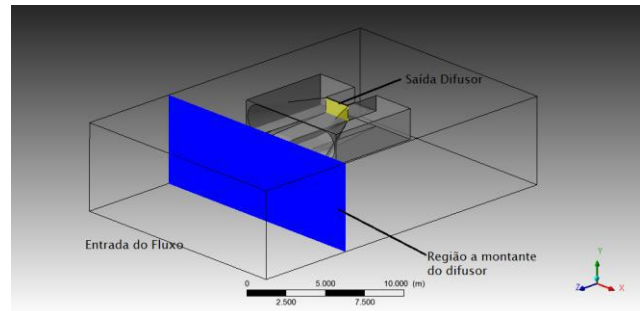


Fig.13: Details of regions to obtain average speeds.

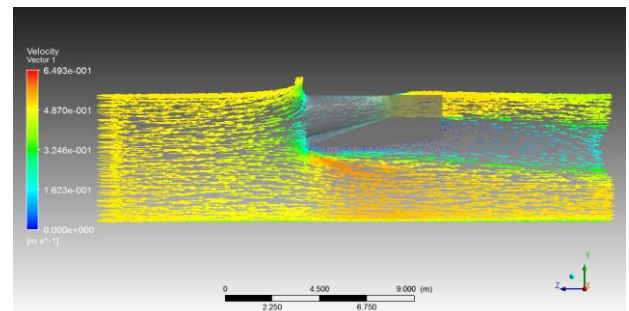


Fig.14: Velocity vectors for input flow of 0.5 m/s

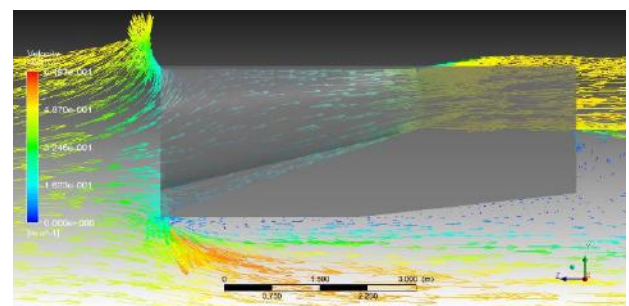


Fig.15: Velocity vector field detail for 0.5 m/s flow.

Figures 14, 15, and 16 show a significant reduction in recirculation below the diffuser.

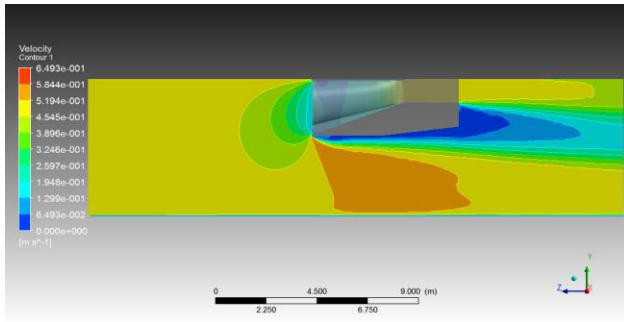


Fig.16: Velocity field for 0.5 m / s flow.

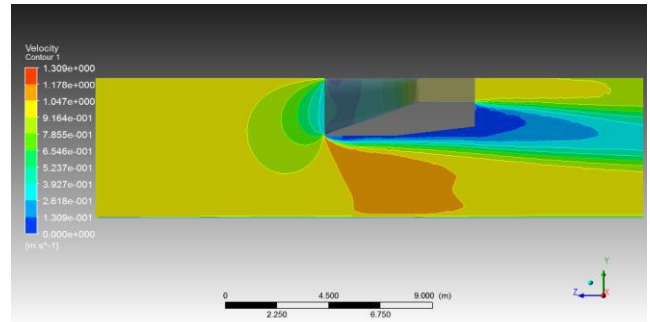


Fig.19: Velocity field for 1.0 m/s flow.

As can be seen, there is a high-velocity region below the diffuser. By the principle of mass conservation, the tendency is for the flow to pass through regions with less obstruction. Nevertheless, we observed a loss of speed along the path (Fig.16); however, we observed that the diffuser played its role, increasing the rate at its exit. The figures below show different velocity profiles in the equipment as a function of different initial flow velocities.

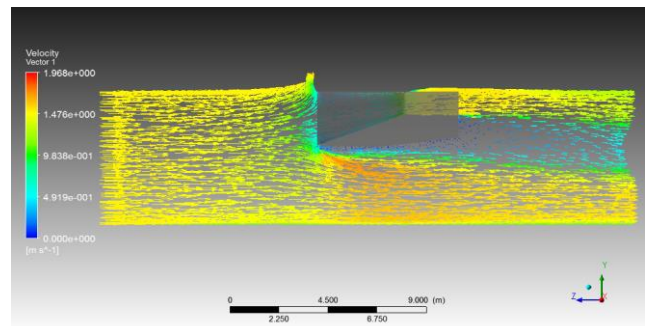


Fig.20: Velocity vectors for the input flow of 1.5 m/s.

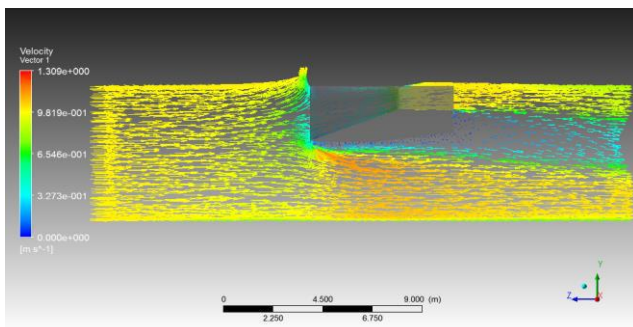


Fig.17: Velocity vectors for input flow of 1.0 m/s.

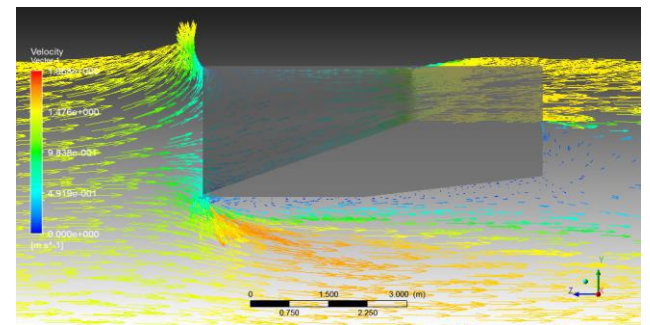


Fig.21: Velocity vector field detail for 1.5 m/s flow.

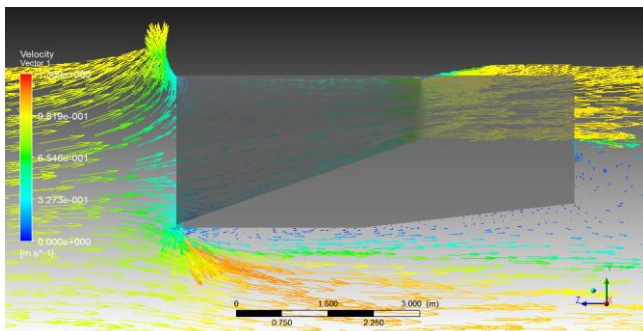


Fig.18: Velocity vectors for input flow of 1.0 m/s.

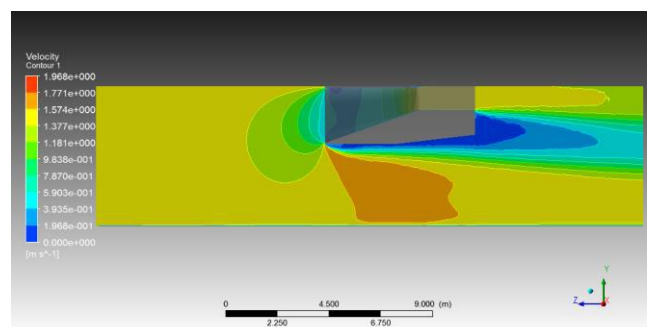


Fig.22: Velocity field for 1.5 m/s flow.

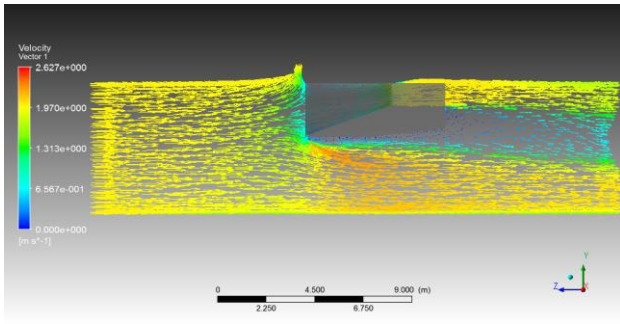


Fig.23: Velocity vectors for the 2.0 m/s input flow.

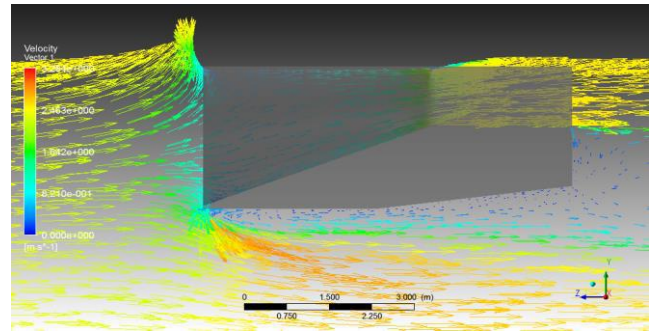


Fig.27: Velocity vector field detail for 2.5 m/s input flow.

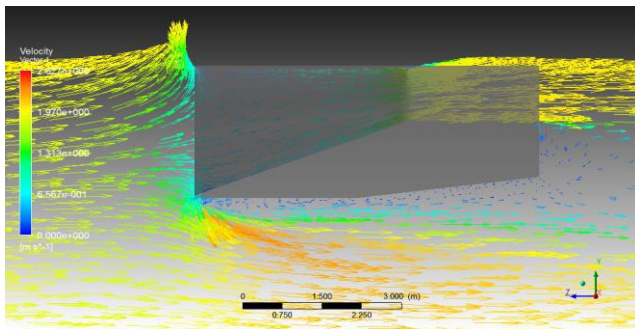


Fig.24: Velocity vector field detail for 2.0 m/s input flow.

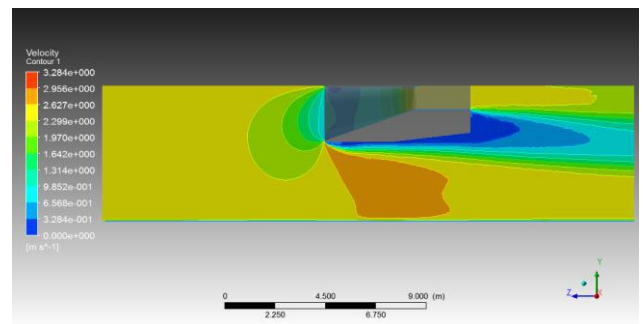


Fig.28: Velocity field for 2.5 m/s flow.

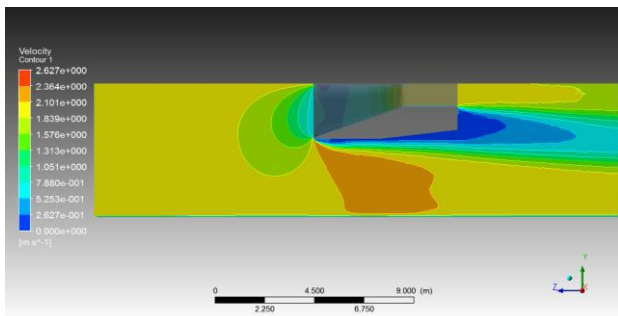


Fig.25: Velocity field for 2.0 m/s flow.

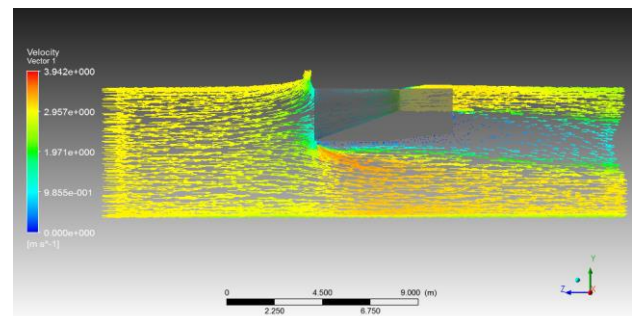


Fig.29: Velocity vectors for input flow of 3.0 m/s.

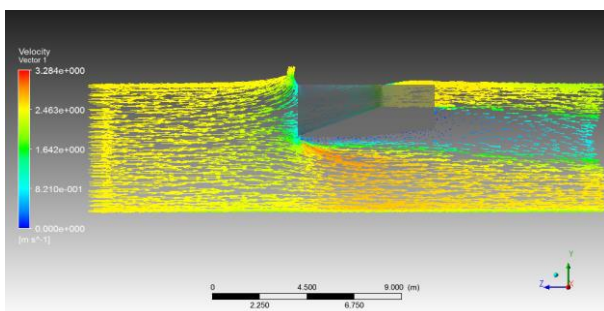


Fig.26: Velocity vectors for input flow 2.5 m/s.

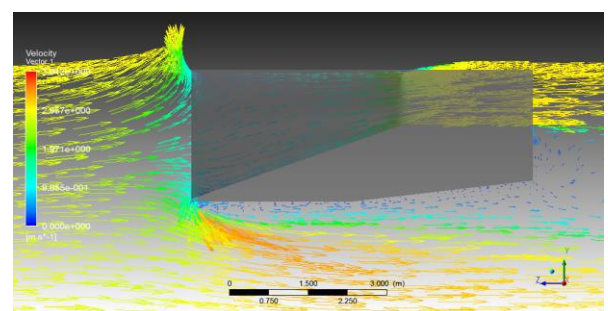


Fig.30: Velocity vector field detail for 3.0 m/s input flow.

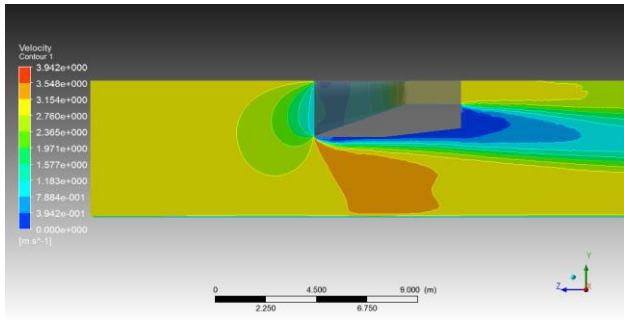


Fig.31: Velocity field for 3.0 m/s flow.

The model presented will be printed (3D printer) in reduced scale for testing in the Control and Automation laboratory channel to validate numerical results. As only the flow of the Madeira River is known, through the simulation, an average rotation that would be produced by the flow passing through the diffuser was estimated. We will use this rotation to simulate both the electrical and mechanical parts of the rotor to obtain the shaft torque produced in the turbine.

It determined an average rotation of the average speed at the diffuser output. Considering that the rotor blade is 1 m long and the linear velocity is proportional to the angular velocity:

$$V = \omega R \tag{1.0}$$

Table 2 presents the values of the theoretical average rotation obtained from the average output speed of the rotor.

Table 2: Theoretical average rotation obtained at the diffuser output

Input	Average Rotation (r.p.m.)
3,0	57,26865951
2,5	47,70312912
2,0	38,14237338
1,5	28,58581933
1,0	19,03495666
0,5	9,495037482

This average rotation will be used in the modeling of the electrical part and the simulation of the rotating part of the turbine (rotor).

The generator's electrical machine can either be built with permanent magnets or a squirrel-cage induction motor, and the voltage generated varies according to the installation's water flow. A proprietary conversion system,

built into the system body, synthesizes frequency and voltage to desired values. This generation system will be made with permanent magnets.

Considering the movement of the permanent magnet rotor, the distance traveled by a pair of magnets induces a voltage cycle at the terminals of a stator coil taken as a reference. Thus, adopting thirty magnets on the concentric segment of magnetizable material, adjacent to the face with fixed magnets, spaced by a few millimeters, there will be another concentric segment for the mechanical support of the nine stator units, generating different phases of electrical voltage.

Due to the initial perspective of adopting three concentric stators in the full-scale design, there would be different tangential speeds for the same rotor speed. A fact that inevitably conditions the design of the coils to three distinct types. In the smaller-scale design, each of these three stator coil designs is on a single circle. There should be different assessment criteria, adopting three speeds for each test.

The rotation speeds in the reduced-scale prototype will be such that they must induce voltage at the frequencies of 35.2 Hz, 29.4 Hz, and 25.2 Hz, respectively, those observed in the full-scale model design, from the most external stator to the more internal.

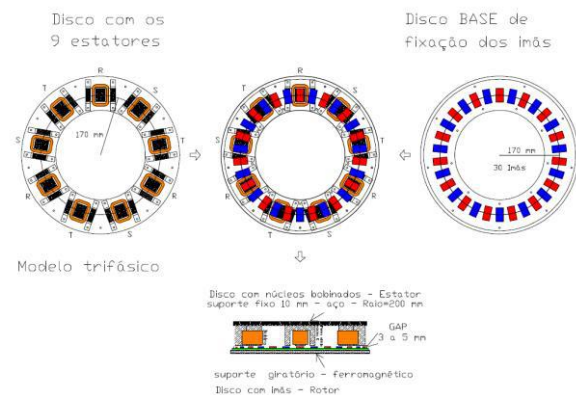


Fig.32: Small-scale prototype stator and rotor.

Considering that the passage of a pair of magnets from different magnetic poles induces an electrical voltage cycle at the unit stator terminals taken as a reference, considering the rotor with 30 magnets, for those steady-state frequencies, follows the proportion below:

$$\begin{matrix} (35,2 \text{ Hz}) \\ (29,4 \text{ Hz}) \\ (25,2 \text{ Hz}) \end{matrix} \text{ ————— } (X) \text{ magnets} \tag{2.0}$$

$$1 \text{ Hz} \text{ ————— } 2 \text{ magnets}$$

Therefore:

$$X = \begin{pmatrix} 70,4 \\ 58,8 \\ 50,4 \end{pmatrix} \text{ magnets/s} \tag{3.0}$$

Thus, the steady-state will be reached from the outermost to the innermost stator in the full-scale model. There are displacement rates of 70.4, 58.8, and 50.4 magnets per second.

Considering the model at a minimum scale with one circular path that containing the thirty magnets, the necessary velocities for each of the three different stator units to reach the steady-state will be obtained with the proportion below:

$$\begin{pmatrix} 70,4 \\ 58,8 \\ 50,4 \end{pmatrix} \text{ magnets/s} \xrightarrow{\hspace{10em}} 1 \text{ rev/s}$$

$$30 \text{ magnets/s} \xrightarrow{\hspace{10em}} \begin{pmatrix} 2,35 \text{ rev/s} = \frac{2,35 \text{ RPM}}{60^{-1}} \cong 141,0 \text{ RPM} \\ 1,96 \text{ rev/s} = \frac{1,96 \text{ RPM}}{60^{-1}} \cong 117,6 \text{ RPM} \\ 1,68 \text{ rev/s} = \frac{1,68 \text{ RPM}}{60^{-1}} \cong 100,8 \text{ RPM} \end{pmatrix} \tag{4.0}$$

The rotations calculated for the model in minimum scale are intended to validate the theoretical and practical arrangement, leading to the refinement of the electrical design of the machine in full scale.

For the best understanding of the study, each of the three stator unit designs will be fixed side by side in a single path of excitation by the rotor. They will be identified as R-phase, S-phase, and T-phase. The values for phases R, S, and T represent the stator rotation on a minimum scale with the same speed of passage of the magnets provided in the full-scale model.

Phase R

- Rotation in steady-state 141.0 r.p.m.;
- Number of turns per stator unit 85 (15 AWG);
- Maximum electrical current in conductors (450 A/cm²) 7,427 A;
- Theoretical value (per stator unit) at 16.0 V steady state rotation.

Phase S

- Rotation in permanent regime 117,6 r.p.m.;
- Number of turns per stator unit 109 (15/16 AWG);
- Maximum electrical current in conductors (450 A/cm²) 5,890 A ;
- Theoretical value (per stator unit) at 17.2 V steady state rotation.

Phase T

- Rotation in steady-state 100.8 r.p.m.;

- Number of turns per stator unit 136 (17 AWG);
- Maximum electrical current of conductors (450 A/cm²) 4,671 A ;
- Theoretical value (per stator unit) at 18.5 V steady-state rotation.

III. PROTOTYPE OF THE HYDROKINETIC GENERATION SYSTEM COUPLED TO THE AXIAL FLOW GENERATOR

The model was printed on a reduced-scale 3D printer for testing in the channel belonging to the Control and Automation laboratory to validate the results presented in the simulation.



Fig.33: Hydrokinetic Power Generation System coupled to the Axial-Flow Generator.



Fig.34: Turbine and diffuser overview.

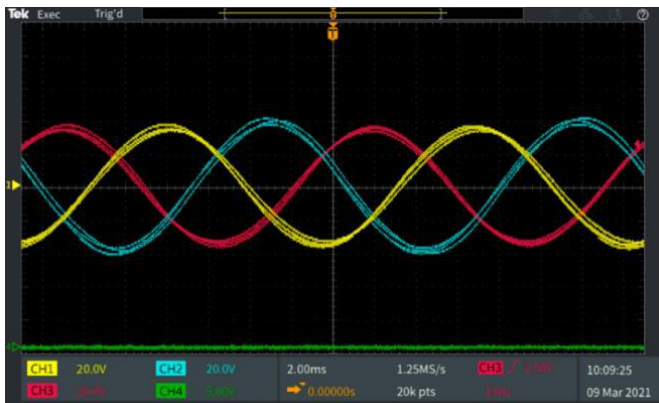


Fig.35: The three-phase voltage generated in loads of 1Ω of 30 W.

IV. CONCLUSION

The new diffuser geometry proposed in this article increased its output speed as predicted in the simulations and the test channel.

The built prototype can generate energy for isolated communities and can be used in various economic activities with rivers, canals, or small watercourses, with low flow speeds.

The proposed system is relevant for its low manufacturing and installation cost. Furthermore, it contributes to the preservation of the environment, as there is no need for dams.

ACKNOWLEDGEMENTS

The authors thank the company EDF Norte Fluminense S.A. and the Technology and Innovation Research Group.

REFERENCES

- [1] Sonia Magalhães dos Santos, Jorge Alberto Almeida, Daniel Alves de Andrade, Leonardo Files Dias Turbina Hidrocinética Axial. Proceedings of the 10o Brazilian Congress of Thermal Sciences and Engineering – ENCIT 2004. Braz. Soc. of Mechanical Sciences and Engineering -- ABCM, Rio de Janeiro, Brazil, Nov. 29 -- Dec. 03, 2004.
- [2] Vermaak, Herman Jacobus; Kusakana, Kanzumba; Koko, Sandile Philip. Status of micro-hydrokinetic river technology in rural applications: A review of the literature. Renewable and Sustainable Energy Reviews, v. 29, p. 625-633, 2014.
- [3] Ricciotti, A. C. D., Ricciotti, V. B. S. D, Militão, J. S. L. T, Steiner, F. M., Medina, F. J., Hydrochemetic Converter Coupled to Axial-Flux Generator in Floating Systems. International Research Journal of Engineering and Technology (IRJET), pages 2252-2267,2019.
- [4] Santos, Ludmila Evangelista dos. Restauração da Turbina Hidrocinética de Primeira Geração Desenvolvida pela Universidade de Brasília: UnB, 2016. 31 p.
- [5] Patente BR 10 2016 013135 9, em 08/06/2016, aguardando conclusão.
- [6] Lima, L.S. Estimativa de vazões para o Canal São Gonçalo, o sistema lagunar Patos-Mirim -RS, através do Método das Velocidades Indexadas. 2016, 63p. Trabalho de Conclusão de Curso (Engenharia Hídrica) - Engenharia Hídrica, Universidade Federal de Pelotas, Pelotas, 2016.